DISTRIBUTION STATEMENT A
Approved for public release;
Distribution Unlimited

SECURITY CLASSIFICATION OF THIS PAGE

REPORT DOCUMENTATION PAGE

DTIC FILE COPY

DTIC ELECTE DEC 09 1988 D JLE

AD-A202 869

1b. RESTRICTIVE MARKINGS	
3. DISTRIBUTION / AVAILABILITY OF REPORT: Distribution Unlimited	
4. PERFORMING ORGANIZATION REPORT NUMBER(S): Ha	5. MONITORING ORGANIZATION REPORT NUMBER(S)
University of California, Irvine	
6a. NAME OF PERFORMING ORGANIZATION: University of California, Irvine	6b. OFFICE SYMBOL (If applicable)
7a. NAME OF MONITORING ORGANIZATION: Office of Naval Research, Code 1511	
6c. ADDRESS (City, State, and ZIP Code): Department of Physiology & Biophysics, D340, Med Sci I, Irvine, CA 92717	7b. ADDRESS (City, State, and ZIP Code): 800 N. Quincy Street, Arlington, VA 22217-5000
8a. NAME OF FUNDING / SPONSORING ORGANIZATION: Office of Naval Research	8b. OFFICE SYMBOL (If applicable)
9 PROCUREMENT INSTRUMENT IDENTIFICATION NUMBER: N00014-87-K-0049	
8c. ADDRESS (City, State, and ZIP Code): 800 N. Quincy Street, Arlington, VA 22217-5000	10 SOURCE OF FUNDING NUMBERS: PROGRAM ELEMENT NO; PROJECT NO; TASK NO; WORK UNIT ACCESSION NO

11. TITLE (Include Security Classification)

Neuromodulation of Ion Channels and Calcium Signaling in T Lymphocytes

12. PERSONAL AUTHOR(S)
Michael Cahalan

13a TYPE OF REPORT	13b. TIME COVERED	14. DATE OF REPORT (Year, Month, Day)	15. PAGE COUNT
Annual	FROM 2/1/87 TO 1/30/90	11/30/88	14

16. SUPPLEMENTARY NOTATION

17. COSATI CODES			18. SUBJECT TERMS (Continue on reverse if necessary and identify by block number)
FIELD	GROUP	SUB-GROUP	
			Ion Channels

19. ABSTRACT (Continue on reverse if necessary and identify by block number)

Ion channels play a crucial role during early periods of lymphocyte activation by mitogens. This project seeks to define the molecular substrates of neural modulation of immunity, using a combination of patch clamp methods to examine ion channels in lymphocytes, and fluorescence imaging to monitor changes in intracellular $[Ca^{2+}]$. Our hypothesis is that neurotransmitters and peptides may influence functional responses of the immune system by modulating properties of ion channels, which in turn regulate several aspects of lymphocyte activation and effector function. Over the past year we have constructed two experimental setups to monitor $[Ca^{2+}]$ inside cells using fura-2, a dye which changes its fluorescence excitation properties when Ca^{2+} binds. We have also further characterized the diversity of channels which occurs in T lymphocytes and demonstrated that the distribution of K^+ channels is subset-specific. These experiments have expanded the list of potential substrates for neural modulation of immunity, and have provided the technical framework for studying ion channels responsible for Ca^{2+} signalling, a cellular response to mitogens crucial for activation.

20. DISTRIBUTION / AVAILABILITY OF ABSTRACT	21. ABSTRACT SECURITY CLASSIFICATION
☒ UNCLASSIFIED/UNLIMITED ☐ SAME AS RPT ☐ DTIC USERS	
22a NAME OF RESPONSIBLE INDIVIDUAL: Michael Cahalan	22b TELEPHONE (Include Area Code): (714) 856-7260 / 22c OFFICE SYMBOL

DD FORM 1473, 84 MAR 83 APR edition may be used until exhausted. All other editions are obsolete.

SECURITY CLASSIFICATION OF THIS PAGE

ANNUAL REPORT
OFFICE OF NAVAL RESEARCH CONTRACT
N00014-87-K-0049
Feb. 1, 1988, Jan. 31, 1989

I. INTRODUCTION

Over the past five years, the patch clamp technique (1) has enabled the study of ion channels in a variety of cells of the immune system. The advantages of patch recording include the ability to record from very small cells, resolution to the level of single ion channels, the ability to control the readily diffusible constituents of cytoplasm, and the ability to study isolated membrane patches in either outside-out or inside-out configurations. We have recently reviewed the types of channels found in cells of the immune system emphasizing the parallels between nervous and immune system channel plasticity during differentiation and activation (2). Several types of ion channels previously characterized in excitable cells such as nerve and muscle are also expressed by cells of the immune system. Tetrodotoxin-sensitive, **voltage-gated Na^+ channels** are infrequently found in lymphocytes (3), but are abundant enough in certain leukemia cell lines (K562, 4) and in mouse natural killer cells to produce action potentials (Cahalan and Sutro, unpublished observations). **Voltage-gated Ca^{2+} channels** with properties similar to inactivating, transient-type Ca^{2+} channels (T in the nomenclature of Dr. Richard Tsien) have been recognized in secreting B-cell hybridomas (5,6), but have not been found in normal lymphoid cells. Several distinct types of K^+ channels have been found in various cells of the immune system. The most abundant type of channel in T lymphocytes is a **voltage-gated K^+ channel** (termed type *n* for *normal*), similar in its biophysical characteristics to K^+ channels in skeletal muscle cells which mediate repolarization of the action potential (3,7-11). Other types of K^+ channels - including **inward rectifier K^+ channels that turn on when the membrane is made more negative**, and **Ca-activated K^+ channels** that turn on when intracellular $[Ca^{2+}]$ rises - have not been seen in lymphoid cells, but are expressed in other cells of the hemopoietic lineage (12-14).

A few types of channels have been discovered in lymphoid cells. Two variants of **voltage-gated K^+ channels, n' and l**, have been recognized in murine cytotoxic/suppressor T cells (15-18). Two types of **Cl^- channels**, one of which may play a role in the regulation of cell volume, have been characterized in lymphocytes (19). Ca^{2+} channels have proved more elusive, although a **nonselective, Ca^{2+}-permeable channel** has been identified at the single channel level (20). This channel has an increased opening probability in the presence of IP3 (21), and could represent the Ca^{2+} entry pathway stimulated early in mitogenesis, although this has not been tested. Toward the goal of further characterizing the ion selectivity, gating and pharmacology of mitogen-regulated Ca^{2+} channels, we have recently identified a divalent-selective current in whole cell recordings.

Channel phenotype and function. Within the hematopoietic cell lineage, we have recorded from red blood cells, platelets, neutrophils, T and B lymphocytes, basophilic cells, hybridomas, and several types of leukemic cells. Each cell type appears to express its own unique contingent of ion channels, suggesting that channels may contribute to the functional capability of various cell types. For example, Hagiwara's lab has shown that expression of voltage-gated Ca^{2+} channels parallels the ability to secrete antibodies in B-cell hybridoma cell lines, suggesting that Ca^{2+} channels play a role in antibody secretion (5). Reuter's group has identified a nonselective cation channel that is permeable to Ca^{2+} ions and would appear to amplify the calcium signal in neutrophils stimulated with chemotactic peptide (22). The nonselective, Ca^{2+}-permeable channels in T cells, studied by Gardner and colleagues, become closed when $[Ca^{2+}]_i$ rises, an effect which may limit

the Ca^{2+} rise. The role of ion channels is unclear regarding macrophage functions, examined by Gallin's group, and degranulation by mast cells and basophils, studied by Neher, Almers, Fernandez, and colleagues (23-25). Evidence from our lab, as well as from Deutsch, McKinnon, Hagiwara and their colleagues, relating K^+ channels in T lymphocytes to mitogenesis and cytotoxicity is briefly summarized next.

K^+ channels and T-cell activation. Voltage-gated K^+ channels appear to be essential for T-lymphocyte activation. Mitogenic lectins enhance the opening of K^+ channels in a rapid and irreversible effect, resulting in membrane hyperpolarization and increased K^+ efflux (3,26,27). By comparing the dose-response relation of channel block by a variety of agents (summarized in Table 1) with that for immunological and biochemical assays of events in T-cell activation, we have shown that K^+ channels are required for mitogen-stimulated thymidine uptake, protein synthesis, and IL-2 production, but not for expression of the IL-2 receptor (22). Furthermore, functioning K^+ channels are required for target cell lysis by activated cytotoxic T cells and natural killer cells (4). In order to exclude nonspecific cytotoxic effects of K^+-channel blockers, three types of control experiments were performed (7,28). First, T lymphocytes incubated with blockers were viable by the criterion of trypan blue dye exclusion. Second, normal incorporation of ^{3}H-thymidine was observed after washing out the blockers, indicating that inhibition was not due to general toxicity. Third, the blockers did not inhibit ^{3}H-thymidine incorporation in a cell line that lacks K^+ channels, CCRF-HSB-2. K^+-channel blockers inhibit mitogenesis measured at 60 hours, only if they are added during the first 20-30 hours of mitogen stimulation (28,29). This implies that the K^+ channel is required for some early event(s) in T-cell activation.

II. PROGRESS REPORT

Overview of ion channels found. We have further characterized the biophysical and pharmacological properties of voltage-gated K^+ channels. By examining the influence of divalent ions, we provided additional evidence that these channels are not activated by Ca^{2+}, but that divalent ions can be trapped inside the K^+ channel. We discovered that different varieties of voltage-gated K^+ channels are expressed by T-lymphocyte subsets. We also discovered two types of Cl^- channels, one of which can be opened by osmotic stimuli. In whole-cell recording, we have identified a divalent-selective conductance which may provide the influx pathway for Ca^{2+} ions following mitogen stimulation. We have correlated the appearance of Ca^{2+} channels with measurement of intracellular $[Ca^{2+}]$ using the indicator dye, fura-2. These results are summarized below. Two channel types that we and several other groups have *not* found in T cells are voltage-gated Ca^{2+} channels and Ca^{2+}-activated K^+ channels, such as the "maxi-K" channel.

K^+ channel pharmacology. One striking aspect of K^+ channels in T lymphocytes is that they can be blocked by a wide variety of agents, including those known to have effects on calcium channels and calcium-activated channels in other types of cells. This wide spectrum of pharmacological sensitivity is intriguing, perhaps suggestive of an underlying structural relatedness among channels - possibly a channel superfamily. In addition, the blocking compounds provide tools to assess the involvement of K^+ channels in T-cell functions. Two of the recently discovered blockers merit special note. Charybdotoxin, a component of *Leiurus* scorpion venom, blocks T lymphocyte K^+ channels with an apparent Kd of 300 pM, a sensitivity which may facilitate biochemical characterization of lymphocyte K^+ channels.

In collaboration with Dr. Patricia Schmidt, a member of the Ob-Gyn faculty at UCI, I have tested several steroid hormones for effects on ion channels in T cells. Dr. Schmidt's research interests include how the immune system functions during pregnancy.

Progesterone blocks K^+ channels reversibly with a threshold effect at ~1 ug/ml. Dr. Schmidt has also found that the Ca^{2+} signal and mitogen-stimulated ^{3}H-thymidine uptake are inhibited at similar doses of progesterone. Higher concentrations are found in the placenta, raising the possibility that progesterone acts locally in the placenta to block lymphocyte K^+ channels and mediate a transient, localized immunosuppression. This mechanism might serve to protect the fetus from attack by the mother's T cells, without inhibiting immune responsiveness in the mother's circulation. We may have discovered an endogenous K^+ channel blocker.

Divalent ion trapping inside the K^+ channel. The K^+ channel's gating mechanism is sensititive to calcium and potassium ions. Bregestovski has reported that raising intracellular Ca^{2+} above the physiological range (>1 uM) accelerates the inactivation rate and reduces the whole-cell conductance (30), reinforcing the conclusion that these channels are not calcium-activated (3,7,8). In exploring effects of divalent ions, we found that extracellular Ca^{2+} also enhances the rate of inactivation (8). Recently, we have done experiments to determine whether this effect is due to Ca^{2+} ions passing through K^+ channels, analogous to Ca-induced inactivation of Ca^{2+} channels (31). Raising the intracellular buffering by including 55 mM BAPTA, a calcium chelator similar to EGTA but with faster kinetics, had no effect on the rate of inactivation. Thus it appears that *the site for Ca^{2+} modulation of inactivation* (K_d = 3.5 mM) is either on the outside surface of the channel or possibly inside the channel, but not inside accessible to internal Ca^{2+} buffer. We found that externally applied Ba^{2+} ions can become trapped inside the K^+ channel; block is relieved after washing only when pulses are given to open the channel. Using Rb ions externally to slow K^+ channel kinetics, we discovered that Ca^{2+} ions can also become trapped inside the K^+ channel, but are apparently released to the cytoplasm in between pulses. This means that Ca^{2+} ions are sparingly permeant in K^+ channels.

Three types of K^+ channels. Our recent studies on T cells and thymocytes from mice support the idea that K^+ channels are required for cell proliferation. During the life of a T cell, expression of type *n* voltage-gated K^+ channels parallels cell proliferation. During differentiation in the thymus, rapidly proliferating immature cells express abundant K^+ channels. As cells mature and become committed to either helper or cytotoxic/suppressor subsets, the number of K^+ channels per cell decreases in the quiescent state. Upon subsequent mitogen stimulation, T cells up-regulate the K^+ channels prior to cell division. The type of K^+ channel in proliferating murine T cells and thymocytes (type *n*) is the same as the K^+ channel in human T cells. We have recently found that two additional types of K^+ channel - called type *l* for *large* conductance or *lpr* (signifying lymphoproliferation), and type *n'* to suggest homology to the normal type channel - are expressed selectively in quiescent $CD8^+$ cells of the cytotoxic/suppressor lineage. Mitogen-unresponsive T cells from diseased MRL-*lpr* mice also express primarily type *l* K^+ channels. Thus, the type of K^+ channel expressed varies according to the functional class and proliferative state of the T cell. This pattern of expression is suggestive of a functional role, and can be used as a marker for differentiation and pathology.

Channel expression in thymocytes and mature splenic T cells. We have used a combination of patch clamping and fluorescence microscopy to correlate ion channel expression with the differentiation of T lymphocytes within the thymus (18). Fluorescently labeled monoclonal antibodies were used to visualize two surface antigens, CD4 and CD8, that are expressed in mature helper T cells, and suppressor/cytotoxic T cells, respectively. These antigens participate in MHC recognition. (CD4 is also the AIDS virus receptor.) The double negative and double positive cells proliferate rapidly *in vivo*, and thus occurrence of large numbers of type *n* channels in these cells is consistent with a role for type *n* channels in allowing normal T lymphocytes to enter the G_1 phase of the

cell cycle. K+ channel expression was strikingly different in mature thymocytes (18). Thymocytes with the helper T-cell phenotype (CD4+, CD8-) were found to have small numbers of type n channels, whereas cells with the cytotoxic and suppressor phenotype (CD8+, CD4-) expressed moderate to large numbers of type l or n' K+ channels. In mature splenic T lymphocytes, the subset dependence of K+ channel expression is maintained, although with fewer channels per cell expressed. Within 24 hours of adding Con A, the number of K+ channels per mouse T cell increases by about an order of magnitude (16), due entirely to a selective increase in the number of type n K+ channels.

Type l K+ channels provide a marker for abnormally proliferating T cells. MRL-lpr/lpr mice, which carry the lpr (denoting lymphoproliferation) gene mutation, spontaneously develop hyperplasia of phenotypically and functionally abnormal T cells by about the fourth month of age, along with a disease resembling human systemic lupus erythematosus (32,33). T cells from sick MRL-l mice do not respond to mitogens and antigens (34,35). If functional K+ channels are required for T-lymphocyte activation, the deficient mitogenic responses in T cells from MRL-l mice may be associated with altered K+ channels. T cells from diseased MRL-l mice (> 4 months of age), 90% of which are phenotypically and functionally abnormal (36-40), have about 20-fold more K+ channels per cell (200-300 channels/cell), which are nearly all type l (17), in contrast to activated normal T cells which express large numbers of type n channels. Although the primary defect in the disease has not yet been identified, it has been proposed that it involves the aberrant expansion of a subset of immature thymocytes. If true, it is tempting to speculate that this subset is one which gives rise to CD8+ CD4- T cells during normal development. We have recently extended this approach, by examining T cells from a different genetic defect - gld for generalized lymphoproliferative disorder - a developmental disorder which results in an expansion of a similar T cell subset. Again, lymph node T cells in the diseased mice expressed large numbers of type l channels (41). Type l channels may provide a useful surface marker to follow the disease process and the normal differentiation of T cells.

Measurement of intracellular [Ca2+]. T-cell mitogens such as PHA or antibodies to the T-cell receptor/CD3 complex induce a rapid increase in cytosolic calcium, which is believed to be linked to subsequent biochemical events leading to proliferation. To determine the [Ca2+]i signal in individual cells we have added a photomultiplier photon counting detection system to one of the patch clamp setups for simultaneous measurement of patch clamp currents and Fura-2 fluorescence ratios. Software has been written for simultaneous data acquisition of membrane currents and photomultiplier signals. With alternate illumination at 340 and 380 nm (currently done rapidly by movement of a filter cube with appropriate interference filters) we collect data at both wavelengths and then compute the ratio, to estimate [Ca2+]i. To visualize the [Ca2+]i in a population of cells, we have constructed a state-of-the-art imaging facility (diagrammed below) to enable us to study intracellular ion concentrations in individual cells, and to use video-enhanced differential interference contrast optics for extremely high magnification. Combining the fura-2 ratio calcium signal with patch recording will provide a powerful approach to study the mechanism of voltage- and mitogen-dependent calcium entry, as well as modulation of the calcium signal by second messengers. Video imaging provides a dramatic way of observing [Ca2+]i in individual cells. Summarized briefly below and in Figures of the Appendix are some of our results on the mechanism of Ca2+ signalling.

Application of PHA to Jurkat cells induced repetitive oscillations in intracellular Ca2+ that commenced after a delay of 100-300 sec (Fig. 1). Peak Ca2+ values reached micromolar levels in individual cells, and the oscillations occurred with a period of 92 + 12 sec (n=62 cells). This period was not correlated with the response latency. These characteristics of single-cell responses differ markedly from the ensemble average

response; the average response has a sigmoidal onset and reaches a peak level of only 350 nM, with no indication of oscillations. These differences may be explained by the variable latencies of individual cells, their lack of synchrony, and the fact that only ~80% of the cells responded to PHA. The mitogen-evoked Ca^{2+} oscillations in Jurkat cells appear to depend critically on Ca^{2+} influx across the plasma membrane. Reducing extracellular Ca^{2+} to nominally Ca^{2+}-free levels rapidly suppressed the Ca^{2+} rise, with no indication of continuing oscillations (Fig. 2). These results suggest that the oscillations depend on Ca^{2+} influx, perhaps through Ca^{2+} channels. Membrane depolarization by 160 mM K^+_o or application of 5 mM Ni^{2+} also effectively suppressed Ca^{2+} oscillations, suggesting that the Ca^{2+} channels are not activated by depolarization and are blocked by Ni^{2+}.

Whole-cell voltage-clamp experiments were conducted to search for Ca^{2+} channels that are activated by mitogens. We found, surprisingly, that a voltage-independent Ca^{2+} conductance becomes activated spontaneously during whole-cell recording, with properties that strongly suggest that it underlies the response to mitogen. Shortly after "break-in" to the whole-cell recording mode, inward Ca^{2+} current appears (Fig. 3). With time, the influx of Ca^{2+} saturates the Ca^{2+} buffer (EGTA) supplied to the cell's interior from the pipette, and $[Ca^{2+}]_i$ begins to rise. After the $[Ca^{2+}]_i$ exceeds ~200 nM, Ca^{2+}-activated K^+ channels begin to open, creating an outward current that sums with the inward Ca^{2+} current (Fig. 3B). The Ca^{2+} conductance is not voltage-dependent, and influx through the channels is inhibited by depolarization, similar to the results on intact cells described above. Likewise, the Ca^{2+} current is abolished reversibly by 5 mM Ni^{2+}, suggesting that it underlies the Ca^{2+} oscillations evoked by PHA. In some cases, Ca^{2+} current fluctuated, giving rise to $[Ca^{2+}]_i$ and K^+ current oscillations (Fig. 4). Each $[Ca^{2+}]_i$ oscillation was preceded by a transient increase in Ca^{2+} current (Fig. 4B). Analysis of ramp currents during the oscillations demonstrated that while Ca^{2+} current fluctuations precede changes in Ca^{2+} concentration, the Ca^{2+}-activated K^+ current follows the time course of $[Ca^{2+}]_i$ very closely (Fig. 4D). One possible function for the K^+ current may be to maintain a negative membrane potential necessary to maximize Ca^{2+} influx through the Ca^{2+} channels.

Maxi- and mini- Cl- channels and volume regulation. Two novel types of chloride channels have been discovered in patch-clamp studies of lymphoid cells. Kolb and Schwartz originally described an extremely large-conductance channel in macrophages (42), which has since been observed in muscle and epithelial cells (43-45), and in B-cell hybridoma cells (46). We call this channel the "maxi-Cl" channel in honor of its largest conductance state - 400 pS. This channel appears to be dormant normally, but can be induced to conduct in T cells if the membrane is held depolarized to +20 mV for about 2 minutes. The possible functions of this channel are unknown. Recently, we have discovered a second type of Cl^- channel with very different biophysical and induction characteristics - a "mini-Cl" channel so named for its very small single channel conductance ~2 pS. This channel also appears to be dormant normally, but can be induced by osmotic gradients tending to swell the cell, provided that ATP is in the pipette solution. Cl^- conductances can reach quite large values of several nS/cell, representing on the order of a thousand mini-Cl^- channels. We believe that activation of mini-Cl^- channels provides the initial trigger for the regulatory volume decrease (RVD) upon exposure to hypotonic saline, as discussed more fully in manuscript # 8 of the Appendix. The ability of lymphocytes to regulate their volume in the face of osmotic gradients is essential to their proper function in regions such as the kidney, and is also a property shared by several other mammalian cells. RVD is associated with increased K^+ and Cl^- fluxes through separate pathways. From the pharmacology of the RVD response in comparison to the K^+ channel pharmacology outlined in Table 1, it appears that voltage-gated K^+ channels are the pathway for K^+ efflux (8,19,47). The "mini Cl" channel can be

activated by hypotonic solution, perhaps via membrane stretch, and probably represents the anion pathway in RVD, based upon a comparison of ion selectivity of RVD (47) and the mini-Cl^- channel. This conductance must be considered when designing experiments to search for Ca^{2+} channels.

III. PUBLICATIONS (Year 2)

1. Lewis, R.S. and M.D. Cahalan 1988. Subset-specific expression of potassium channel expression in developing murine T lymphocytes. *Science* 239:771-775. (cover illustration)

2. Lewis, R.S. and M.D. Cahalan 1988. The plasticity of ionic channels: parallels between the nervous and immune systems. *Trends in Neuroscience* 11:214-218.

3. Cahalan, M.D. and R.S. Lewis 1988. Role of K^+ and Cl^- channels in T lymphocyte volume regulation. In: R. Gunn, J. Parker (Eds.), **Cell Physiology of Blood**, pp. 282-301.

4. Grissmer, S., M.D. Cahalan, and K.G. Chandy 1988. Abundant expression of type *l* K^+ channels: a marker for lymphoproliferative diseases? *Journal of Immunology* 141:1137-1142.

5. Grissmer, S. and M.D. Cahalan 1989. Divalent ion trapping inside potassium channels of human T lymphocytes. *Journal of General Physiology* in press.

6. Grissmer, S. and M.D. Cahalan 1989. Open K^+ channels of human T lymphocytes that are blocked by TEA cannot inactivate. *Biophysical Journal* in press.

Abstracts

1. Cahalan, M.D. and R.S. Lewis 1987. Ion channels in T lymphocytes: role in volume regulation. *Journal of General Physiology* 90: 7a.

2. Lewis, R.S. and M.D. Cahalan 1987. Diversity of K^+ channel expression in developing T lymphocytes. *Journal of General Physiology* 90: 27a.

3. Sands, S.B., R.S. Lewis and M.D. Cahalan 1988. Charybdotoxin blocks voltage-gated K^+ channels in T lymphocytes. *Biophysical Journal* 53: 260a.

4. Grissmer, S and M. Cahalan 1988. Ba^{2+} and Ca^{2+} trapped inside the K^+ channels of human T lymphocytes. *Biophysical Journal* 53: 260a.

5. Lewis, R.S. and M.D. Cahalan 1988. Voltage-dependent calcium signalling in single T lymphocytes. *Society for Neuroscience Abstracts*

6. Lewis, R.S. and M.D. Cahalan 1988. Single cell measurements of intracellular free calcium in mitogen-stimulated human T lymphocytes. *Society of General Physiologists abstracts*

IV. REFERENCES

1. Hamill OP, Marty A, Neher E, Sakmann B, Sigworth FJ: *Pfluegers Arch.* 391: 85 (1981)
2. Lewis, R.S. and M.D. Cahalan: *Trends in Neuroscience* 11:214 (1988)
3. Cahalan MD, Chandy KG, DeCoursey TE, Gupta S: *J. Physiol.* 358:197 (1985)
4. Schlichter L, Sidell N, Hagiwara S: *Proc. Natl. Acad. Sci. USA* 83:451 (1986)
5. Fukushima Y, Hagiwara S, Saxton RE: *J. Physiol.* 355: 313 (1984)
6. Fukushima Y, Hagiwara S: *J. Physiol.* 358: 255 (1985)
7. DeCoursey TE, Chandy KG, Gupta S, Cahalan MD: *Nature* 307:465 (1984)
8. DeCoursey TE, Chandy KG, Gupta S, Cahalan MD: *J. Neuroimmunol.* 10:71 (1985)
9. Chandy KG, DeCoursey TE, Cahalan MD, Gupta S: *J. Immunol.* 135 787s (1985)
10. Matteson DR, Deutsch C: *Nature* 307:468 (1984)
11. Fukushima Y, Hagiwara S, Henkart M: *J. Physiol.* 351:645 (1984)
12. Gallin EK, Sheehy PA: *J. Physiol.* 369:475 (1985)
13. Lindau M and Fernandez J: *J. Gen. Physiol.* 88:349 (1986)
14. Gallin EK: *Biophys. J.* 46:821 (1984)
15. DeCoursey TE, Chandy KG, Gupta S, Cahalan MD: *J. Gen. Physiol.* 89:379 (1987)
16. DeCoursey TE, Chandy KG, Gupta S, Cahalan MD: *J. Gen. Physiol.* 89:405 (1987)
17. Chandy KG, DeCoursey TE, Fischbach M, Talal N, Cahalan MD, Gupta S: *Science* 233:1197 (1986)
18. Lewis, RS and Cahalan MD: *Science* 239:771 (1988)
19. Cahalan, M.D. and R.S. Lewis 1988. In: R. Gunn, J. Parker (Eds.), **Cell Physiology of Blood**, pp. 282-301.
20. Kuno M, Goronzy J, Weyand CM, and Gardner, P: *Nature* 323 (1986)
21. Kuno M, and Gardner P: *Nature* 326:301 (1987)
22. von Tscharner B, Prod'hom B, Baggiolini, and Reuter H: *Nature* 324:369 (1986)
23. Lindau M and Fernandez J: *J. Gen. Physiol.* 88:349 (1986)
24. Breckenridge LJ and Almers W: *Nature* 328: 814 (1987)
25. Almers W and Neher E: *J. Physiol.* 386:205 (1987)
26. DeCoursey TE, Chandy KG, Gupta S, Cahalan MD: *Nature* 307:465 (1984)
27. DeCoursey TE, Chandy KG, Gupta S, Cahalan MD: *J. Neuroimmunol.* 10:71 (1985)
28. Chandy KG, DeCoursey TE, Cahalan MD, McLaughlin C, Gupta S: *J. Exp. Med.* 160:369 (1984)
29. Deutsch C, Krause D, Lee SC: *J. Physiol.* 372:405 (1986)
30. Bregestovski P, Redkozubov A, Alexeev, A: *Nature* 319:776 (1986)
31. Eckert R and Chad JE: *Prog. Biophys. Molec. Biol.* 44:215 (1984)
32. Murphy, ED (1981). In **Immunologic Defects in Laboratory Animals**. Vol. 2. Eds. by Gershwin, M.E., and Merchant, B. Plenum Press, New York. Pg 143.
33. Smith HR, and Steinberg AD: *Ann. Rev Immunol.* 1:186 (1983)
34. Wofsy DE, Murphy ED, Roths JB, Dauphince MJ, Kipper SB, Talal N: *J. Exp. Med.* 154:1671 (1981)
35. Altman A, Theofilopoulos AN, Weiner R, Katz D, Dixon FJ: *J. Exp. Med.* 154:791 (1981)
36. Theofilopoulos AN, Eisenberg RA, Bourdon M, Crowell JS, Dixon FJ: *J. Exp. Med.* 149:561 (1979)
37. Lewis DE, Giorgi JV, Warner NL: *Nature* 289:298 (1981)

38. Morse HC, Davidson WF, Yetter RA, Murphy ED, Roths JB, Coffman RL: *J. Immunol.* 129:2612 (1982)
39. Dumont FJ, Habbersett RC, Nichols EA, Treffinger JA, Tung AS: *Eur. J. Immunol.* 13:455 (1983)
40. Dumont FJ, Habbersett RC, Nichols EA: *J. Immunol.* 133:809 (1984)
41. Grissmer, S, MD Cahalan, and KG Chandy: *J. Immunology* 141:1137-1142 (1988)
42. Schwarze W, and Kolb HA: *Pflugers Arch.* 402:281 (1984)
43. Blatz A and Magleby K: *Biophys J.* 43:237 (1983)
44. Krouse ME, Schneider GT, Gage PW: *Nature* 319:58 (1986)
45. Gray PTA, Ritchie JM: *TINS* 9:411 (1986)
46. Bosma MM: *Biophys. J.* 49:413a (1986)
47. Cheung RK, Grinstein S, Dosch H-M, Gelfand EW: *J. Cell. Physiol.* 112:189 (1982)

APPENDIX

TABLE AND FIGURES

SUBSTANCES THAT BLOCK T-CELL K^+ CHANNELS

Classical K Channel Blockers
- Tetraethylammonium (TEA)
- 4-aminopyridine (4AP)

"Ca-activated K^+ Channel Blockers"
- Quinine
- Cetiedil
- Charybdotoxin

Ca^{2+} Channel Blockers
- Diltiazem
- Nifedipine, nimodipine, nitrendipine
- Verapamil
- Polyvalent Cations: La^{3+}, Zn^{2+}, Ni^{2+}, Co^{2+}, Mn^{2+}

Calmodulin Antagonists
- Trifluoperazine
- Chlorpromazine

Steroid Hormones
- Progesterone

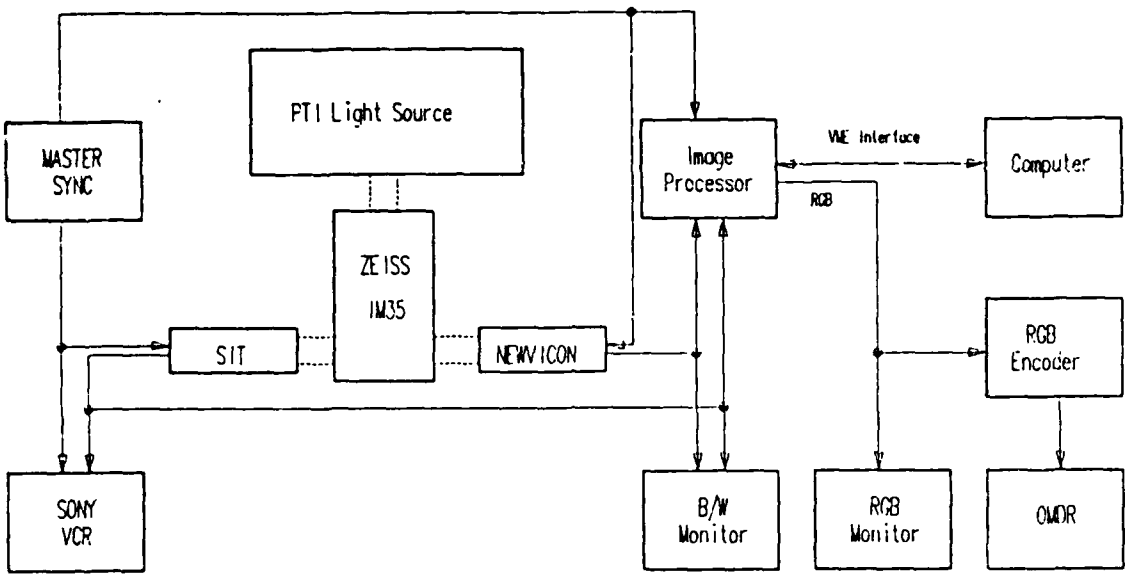

Figure 1. Block diagram of the imaging facility. The microscope is an inverted Zeiss IM35 equipped for epifluorescence and differential-interference-contrast microscopy. Epifluorescence illumination is produced by a computer controlled, dual-monochromator xenon light source (PTI Delta-Scan I). Two video cameras are attached to the microscope: a SIT camera (Dage model 66) for low light level imaging, and a Newvicon camera (Hamamatsu model C2400) for high light level, high-resolution imaging. Both cameras are mounted on optical rails to allow variable magnification of the video image. Prior to image processing, the output of either camera can be observed on a high-resolution black and white monitor and recorded on a computer-controllable video tape recorder (Sony U-Matic VO-9600). The image processor consists of eight VME-based processing modules housed in a remote chassis, controlled by an 80286 personal computer (AST model 170) through an AT-to-VME bus interface (Bit-3). The processing boards (Analog Devices RTI-HS series, designed by Datacube), are arranged in a custom-designed pipeline optimized for real-time fura-2 imaging (i.e., averaging, background correction, and division of video images with zero frame loss). An extensive library of software primitives for controlling processing-board functions have been developed and written in assembly language for optimal speed, by a systems programmer in our laboratory. Processed images are observed on an RGB monitor. Pseudocolored RGB images can be converted to NTSC-compatible video and stored on an optical memory disk recorder (Panasonic TQ-2026F). Horizontal and vertical timing for the entire system is provided by a master sync generator (Grass Valley model 9510).

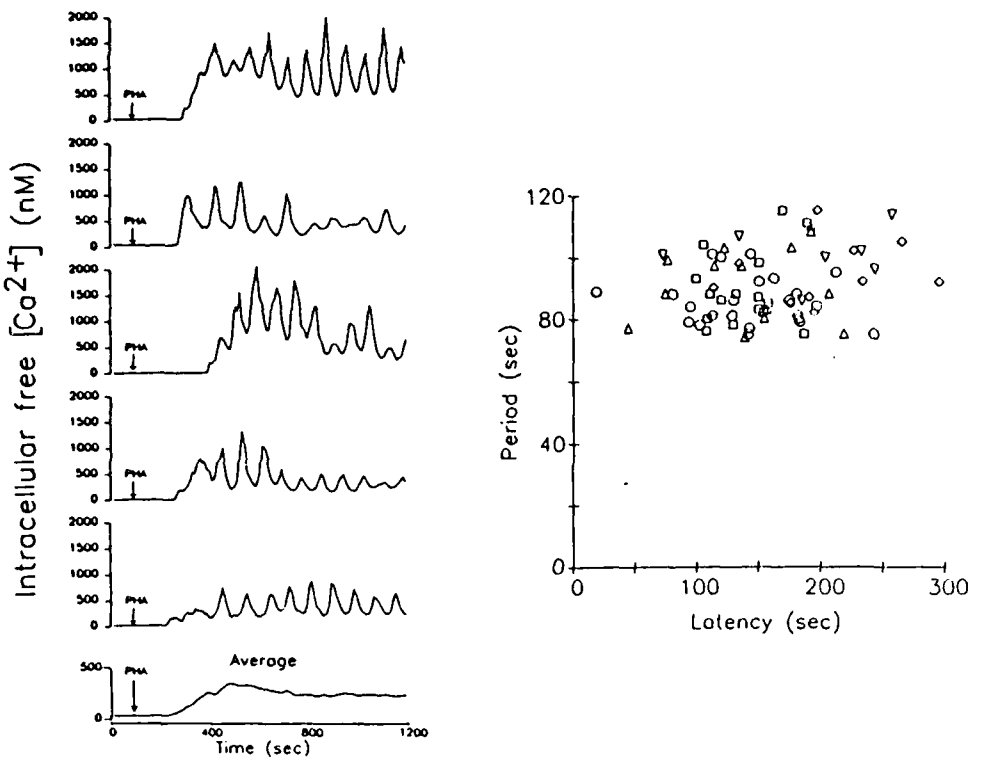

Figure 2. Mitogens evoke $[Ca^{2+}]_i$ oscillations. Jurkat E6-1 human T leukemia cells are loaded with 3 uM fura-2/AM for 30 min at 37°C. Cells are illuminated alternately at 345 and 375 nm and their fluorescence emission at 510 nm collected with a SIT video camera. Sixteen frame averages at each wavelength are divided to yield a ratio image, R. $[Ca^{2+}]$ is then estimated using the equation $[Ca^{2+}]=K_d \cdot S_f (R-R_{min})/(R_{max}-R)$, where S_f, R_{min}, and R_{max} were determined from cells treated with 10 mM EGTA or 10 mM Ca^{2+} in the presence of 5 uM ionomycin. All experiments are conducted at 22-25°C. (LEFT) $[Ca^{2+}]_i$ oscillations evoked in 5 cells by application of PHA (10 ug/ml). The bottom record is the averaged response of 87 cells in this experiment. (RIGHT) The latency of first Ca^{2+} response plotted against oscillation period. Each symbol represents a single cell, and each symbol type represents a different experiment. The period is well-regulated and is not correlated with latency. These results suggest that the rate-limiting step for initiation of the response does not determine the period of the $[Ca^{2+}]_i$ oscillations.

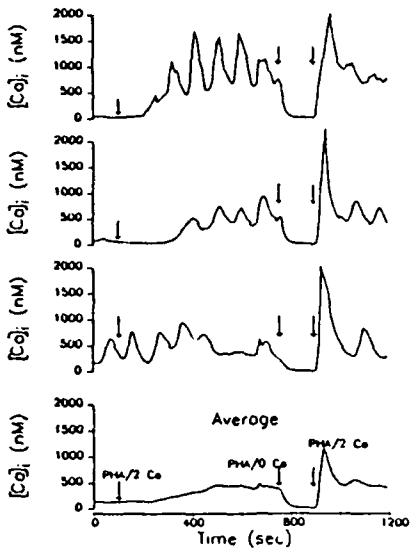

Figure 3. $[Ca^{2+}]_i$ oscillations depend on extracellular Ca^{2+}. The top three traces show responses of single PHA-stimulated cells to removal and restoration of extracellular Ca^{2+}. The average at bottom was obtained from >50 cells in the field of view. At the second arrow, cells were perfused with nominally Ca^{2+}-free PHA solution. Oscillations are suppressed reversibly, suggesting that the PHA response involves Ca^{2+} influx across the plasma membrane.

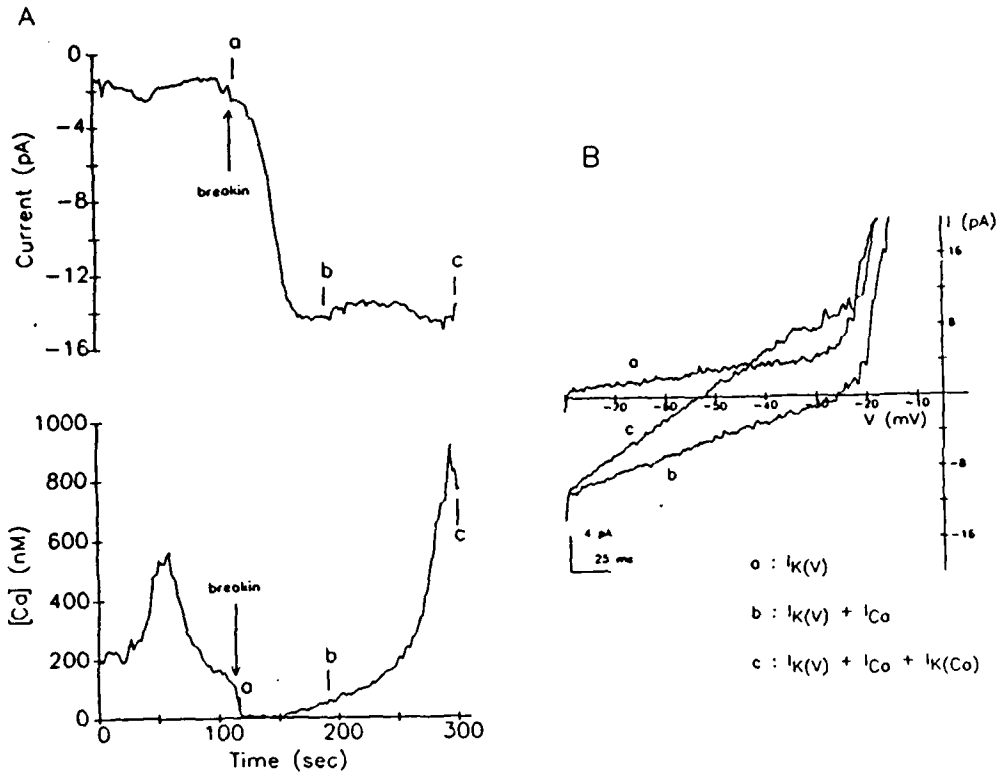

Figure 4. Activation of Ca^{2+} and K^+ currents during whole-cell recording. (A) Changes in inward current at -80 mV (top) and $[Ca^{2+}]_i$ (bottom) occurring shortly after entering whole-cell configuration. EGTA entering the cell from the pipette rapidly chelates the cell's resting Ca^{2+}, but a developing inward current (carrying Ca^{2+} into the cell) eventually saturates the buffer, and $[Ca^{2+}]_i$ rises. (B) Voltage ramps from -80 to 0 mV were applied to distinguish the sequential activation of ion channels during three phases of the recording. Shortly after breakin (a), only voltage-dependent K^+ current is present ($I_{K(V)}$ at V_m > -30 mV). Later (b), an inward Ca^{2+} current develops. As $[Ca^{2+}]_i$ rises (c), a K^+-selective current appears and sums with I_{Ca}; this represents Ca^{2+}-activated K^+ current ($I_{K(Ca)}$).

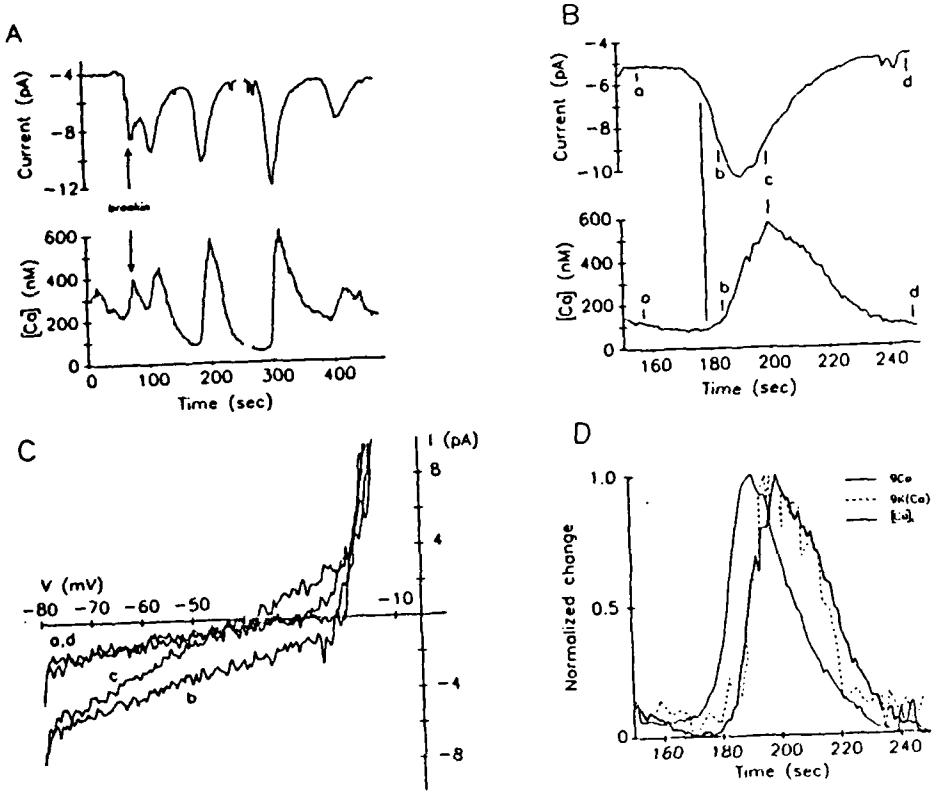

Figure 5. Cyclic activation of Ca^{2+} and K^+ currents during $[Ca^{2+}]_i$ oscillations. (A) Fluctuating inward current measured at -80 mV is associated with repetitive $[Ca^{2+}]$ oscillations. (B) Expanded view of one Ca^{2+} transient from (A). The increase in inward current (arrow) precedes the rise in $[Ca^{2+}]_i$, as expected for a Ca^{2+}-selective current. (C) Four ramp currents collected at times a-d in (B). At time b, an inward Ca^{2+} current has developed. As $[Ca^{2+}]$ rises, K^+ channels become activated (c). After this point, I_{Ca} declines to its initial value, $[Ca^{2+}]_i$ falls, and K^+ channels deactivate (d). (D) Normalized membrane conductances and $[Ca^{2+}]_i$ plotted against time during one oscillation. Conductance values were calculated from ramp currents like those picture in (C). The increase and decrease of g_{Ca} precedes the rise and fall of $[Ca^{2+}]_i$, while $g_{K(Ca)}$ follows the Ca^{2+} transient closely.

DISTRIBUTION LIST

Behavioral Immunology Program

Annual, Final and Technical Reports (one copy each except as noted)

INVESTIGATORS

Dr. Itamar B. Abrass
Department of Medicine
University of Washington
Harborview Medical Center
Seattle, WA 98104

Dr. Prince K. Arora
NICHD, Bldg 6, Room 132
National Institutes of Health
Bethesda, MD 20892

Dr. Karen Bulloch
Helicon Foundation
4622 Sante Fe Street
San Diego, CA 92109

Dr. Michael D. Cahalan
Department of Physiology and Biophysics
University of California, Irving
Irvine, CA 92717

Dr. Donald A. Chambers
Health Sciences Center
University of Illinois at Chicago
P.O. Box 6998
Chicago, IL 60680

Dr. Christopher L. Coe
Department of Psychology
Harlow Primate Laboratory
University of Wisconsin
Madison, WI 53715

Dr. Walla L. Dempsey
Department of Microbiology and Immunology
The Medical College of Pennsylvania
3300 Henry Avenue
Philadelphia, PA 19129

Dr. Adrian J. Dunn
Department of Neurescience
University of Florida
College of Medicine
Gainsville, FL 32610

Dr. David L. Felten
Department of Anatomy
University of Rochester
School of Medicine
601 Elmwood Avenue
Rochester, NY 14642

Dr. John F. Hansbrough
Department of Surgery
UCSD Medical Center
225 Dickinson Street
San Diego, CA 92103

Dr. William F. Hickey
Neuropathology Laboratories
454 Johnson Pavilion
University of Pennsylvania
Philadelphia, PA 19104

Dr. Robert L. Hunter
Department of Pathology
Emory Univ. School of Medicine
WMB 760
Atlanta, GA 30322

Dr. Terry C. Johnson
Division of Biology
Ackert Hall
Kansas State University
Manhattan, KS 66506

Dr. Sandra Levy
University of Pittsburgh
School of Medicine
3811 O'Hara Street
Pittsburgh, PA 15213

Dr. Lester Luborsky
Department of Psychiatry
308 Piersol Building/G1
University of Pennsylvania Hospital
Philadelphia, PA 19104

Dr. Steven F. Maier
Department of Psychology
University of Colorado
Campus Box 345
Boulder, CO 80309

Dr. Michael H. Melner
Department of Biochemistry
Univ of Miami School of Medicine
1600 N.W. 10th Avenue
Miami, FL 33136

Dr. Vera B. Morhenn
Department of Dermatology
Stanford University Medical School
Stanford, CA 94305

Dr. Jose R. Perez-Polo
Gail Borden Bldg., Rm., 436
University of Texas Medical Branch
Galveston, TX 77550-2777

Dr. Howard R. Petty
Department of Biological Sciences
Wayne State University
Detroit, MI 48202

Dr. Bruce S. Rabin
Clinical Immunopathology
Childrens Hospital
University of Pittsburgh Sch of Medicine
Pittsburgh, PA 15213

Dr. Seymour Reichlin
Director, Clinical Study Unit
New England Midical Center Hospitals, Inc.
171 Harrison Avenue
Boston, MA 02111

Dr. Eric M. Smith
Department of Psychiatry
University of Texas Medical Branch
Galveston, TX 77550

Dr. Arthur A. Stone
Department of Psychiatry
State University of New York
at Stony Brook
Stony Brook, NY 11794

Annual, Final and Technical Reports (one copy each except as noted)

ADMINISTRATORS

Dr. Jeannine A. Majde, Code 1141CB (2 copies)
Scientific Officer, Immunology Program
Office of Naval Research
800 N. Quincy Street
Arlington, VA 22217-5000

Administrator (2 copies) (Enclose DTIC Form 50)
Defense Technical Information Center
Building 5, Cameron Station
Alexandria, VA 22314

Administrative Contracting Officer
ONR Resident Representative
(address varies - obtain from business office)

Program Manager
Biological/Human Factors Division
Office of Naval Research, Code 125
800 N. Quincy Street
Arlington, VA 22217-5000

Program Manager
Support Technology Directorate
Office of Naval Technology, Code 223
800 N. Quincy Street
Arlington, VA 22217-5000

Annual and Final Reports Only (one copy each)

DoD ACTIVITIES

Commanding Officer
Naval Medical Command
Washington, DC 20372

Commanding Officer
Naval Medical Research & Development Command
National Naval Medical Center
Bethesda, MD 20814

Director, Infectious Diseases Program Center
Naval Medical Research Institute
National Naval Medical Center
Bethesda, MD 20814

Commander
Chemical and Biological Sciences Division
Army Research Office, P.O. Box 12211
Research Triangle Park, NC 27709

Commander
U.S. Army Research and Development Command
Attn: SGRD-PLA
Fort Detrick
Frederick, MD 21701

Commander - postcard
USAMRIID
Fort Detrick
Frederick, MD 21701

Directorate of Life Sciences
Air Force Office of Scientific Research
Bolling Air Force Base
Washington, DC 20332

Library
Armed Forces Radiation Research
Institute
Bethesda, MD 20814-5145

Final and Technical Reports Only

Director, Naval Research Laboratory (6 copies)
Attn: Technical Information Division, Code 2627
Washington, DC 20375